Electronic Supplementary Material (ESI) for Nanoscale


*Supporting Information*

## 1. Field emission scanning electron microscopy (FE-SEM)

A high resolution SEM image of Ag-doped ZnO NWs exhibited a diameter of about 80 nm and a length of about 1.5 um. Given in this figure, the randomly oriented distribution (not vertically oriented) of Ag-doped ZnO NWs was predominantly attributed to the relatively rough surface morphology of polyester substrates

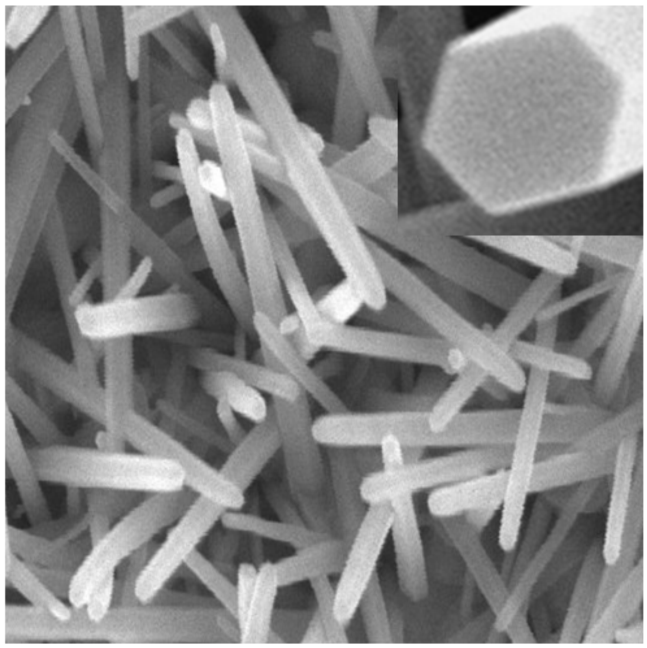

**Fig. S1** SEM image of Ag-doped ZnW NWs on polyester substrate. The inset represents the plan view of single Ag-doped ZnO NW

Fig. S2 displays the tilted SEM images of Ag-doped ZnO NWs grown with various Ag mole concentrations. Seen in fig S2, all the samples exhibited a random growth direction. Uniform synthesis was obtained in a large area, regardless of mole concentrations.

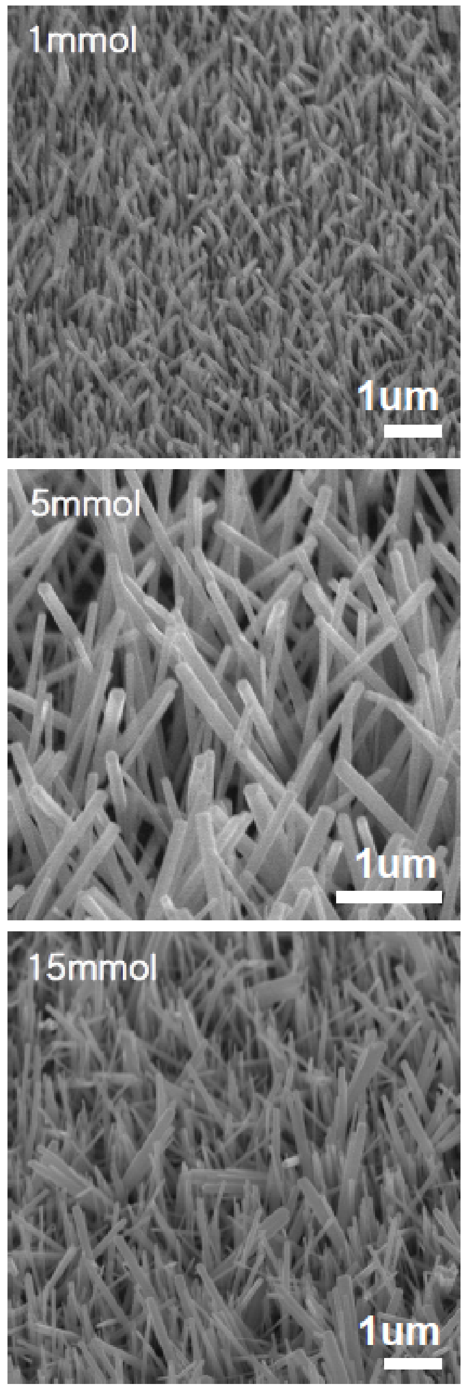


**Fig. S2** SEM image of Ag-doped ZnO NWs grown at various mole concentrations

## 2. Photoluminescence measurement

Fig. S3 demonstrates the low temperature PL spectra of the three Ag-doped ZnO NWs with different Ag dopant source concentrations taken at 10 K. As seen in Fig S3, The intensities of FA peak on Ag-doped ZnO NWs become stronger with decreasing Ag dopant source concentration. This indicates that the Ag-doped ZnO NWs using 1mmol Ag dopant source clearly act as accetor levels which can conpensate the native donors.

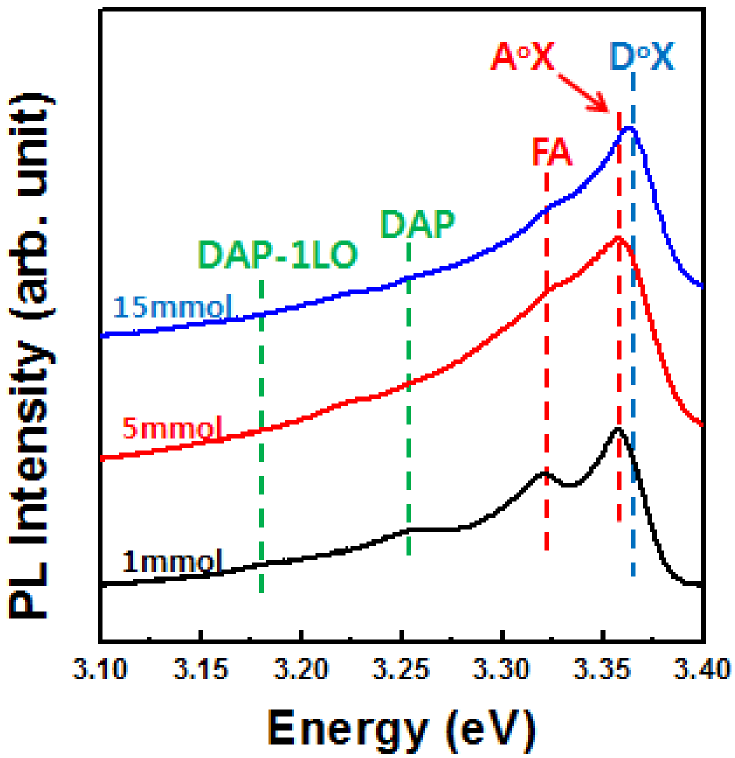


**Fig. S3** PL spectra of Ag-doped ZnO NWs as a function of Ag nitrate mol concentration ranging from 1-15 mmol taken at 10 K

### 3. Varshini fitting

Fig. S4 shows a plot of the experimental and theoretical values of AX over temperature ranging from 10-300 K. The following Varshnis empirical formula was used for the calculation

$$E(T) = E(0) - \frac{\alpha T^2}{T + \beta}$$

where **α** and **β** denote the constants and *E*(0) the energy of each line at T = 0 K. The fit of this model was shown as a solid line (red) through the experimental data points (black). The values of the fit parameters E(0), **α** and **β** were 3.358 eV, 0.001 eV/K and 920 K for the Ag-doped ZnO NWs. The Acceptor bound exciton energy line at 3.357 eV depicted a continuous shift to lower energy as the temperature increased. Theoretical and experimental results for the exciton emission peak displayed a similar temperature dependence trend

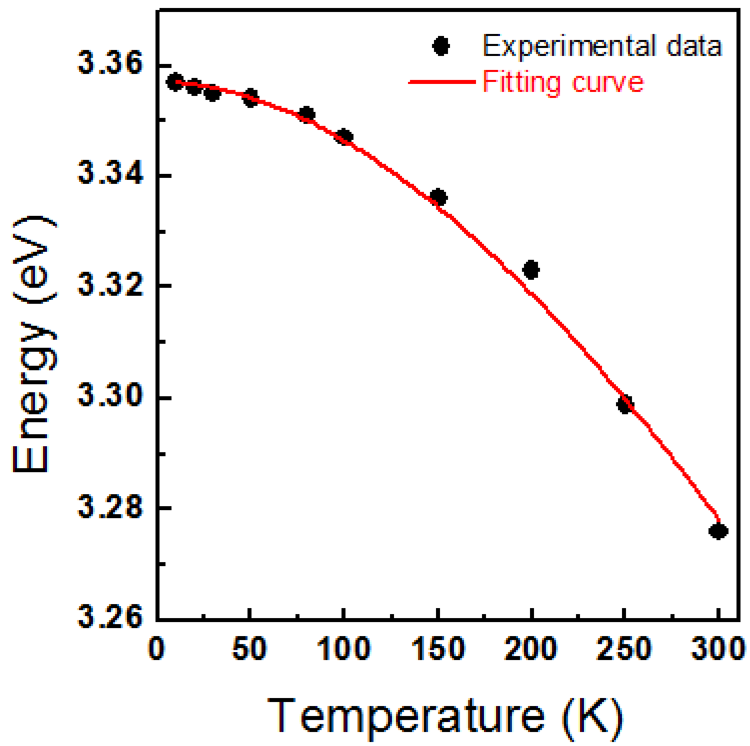


**Fig. S4** Temperature dependence of the transition energy of the $A^oX$ peaks of Ag-doped ZnO NWs, where the solid lines indicate the relative transition energy variation with the Varshni formula.

### 4. The swiching polarity of SPENG

To ensure true signal from Ag-doped ZnO NW nanogenerator, the analysis of switching polarity was performed, as shown in Fig. S5. A swap in electrical connection (forward ↔ reverse) resulted in a reversal in the measured output, demonstrating good agreements in mechanism of piezoelectricity

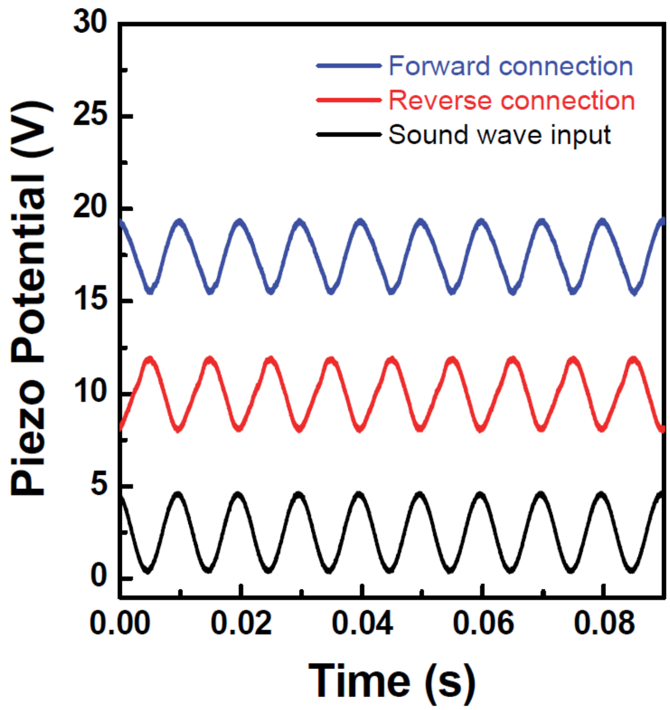


**Fig. S5** Forward (blue line) and reverse (red line) output polarities induced by the sound wave input (black line).

## 5. Rectifying circuits for SPENG

The SPENG were designed to charge the capacitors (100 uF each) with only the switches numbered 1 turned on. Then, the switches numbered 2 and 3 were turned on after the switches numbered 1 turned off. Capacitors were discharged to power the PDLC.

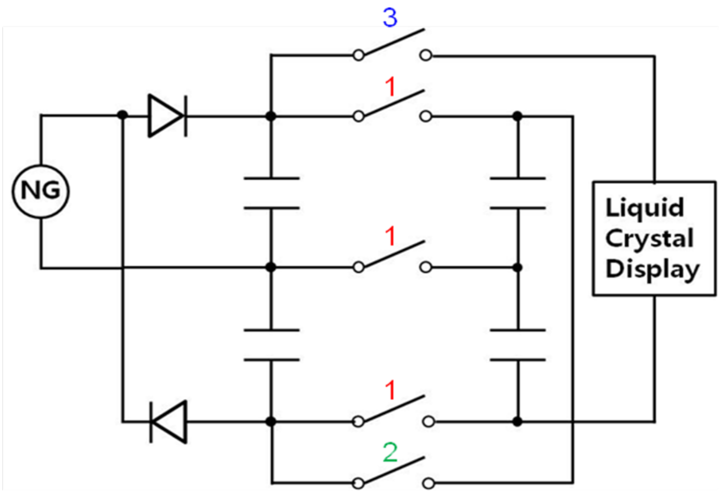


**Fig. S6** Schematic design diagram of the rectifying circuit and charge storage device for Ag-doped ZnO NWs nanogenerato